

GAMMA Simulations of Stray Field Responses: Slice Thickness and Pulse Calibration¹

Paul Kinchesh,* Scott A. Smith,† Alasdair R. Preston,* and Edward W. Randall*

**Department of Chemistry, Queen Mary, University of London, London E1 4NS, United Kingdom; and †National High Magnetic Field Laboratory, Florida State University, Tallahassee, Florida 32310*

Received June 11, 2001; revised October 17, 2001; published online January 16, 2002

A stray field (STRAFI) module has been added to the GAMMA magnetic resonance simulation platform in order to facilitate computational investigations of NMR experiments in large static field gradients that are on the order of 50 T/m. The package has been used to examine system response during echo trains generated by the application of shaped pulses. The associated echo amplitude maxima and effective slice thickness are presented. A new accurate method for STRAFI pulse calibration based on relative echo amplitudes is proposed. © 2002 Elsevier Science (USA)

Key Words: GAMMA platform; simulations; numerical calculations; stray field; STRAFI; fringe field; slice thickness; pulse calibration.

INTRODUCTION

The large magnetic gradients that exist in the fringe field or stray field (STRAFI) of superconducting solenoids range from 10 to 100 T/m in modern NMR spectrometers. These large field gradients have been exploited both to image substances with very broad line shapes at high spatial resolution (1, 2) and to quantify very slow self-diffusion processes (3). In STRAFI imaging applications, sample profiles are typically generated using $\alpha_x\text{-}\tau\text{-}[\alpha_y\text{-}\tau\text{-}echo\text{-}\tau]_n$ echo trains, where α represents the on-resonance pulse flip angle, subscripts x and y represent the relative phases of the pulses, τ is a short time interval of the order of pulse durations, and n is the total number of echoes acquired. The application of short RF pulses in large field gradients excites a narrow slice within the sample about Samoilenko's "sensitive layer" (4), which is typically 10–100 μm thick for protons. Sample profiles are subsequently constructed by the step-wise movement of the sample through the sensitive layer. The slice thickness ultimately defines the spatial resolution of the technique. For narrow lines, the slice thickness is primarily determined by the pulse excitation envelope which, for rectangular pulse shapes, is inherently nonuniform. A quantitative analysis of echo intensities in terms of sample relaxation properties is possible only when the flip angle α is accurately determined (5, 6).

Theoretical analyses of STRAFI echo intensities include the treatments of Benson and McDonald (7, 8) and that of Bain and Randall (9). Benson and McDonald utilized a Bloch treatment and calculated that the maximum amplitude of the first echo occurred at a flip angle of "approximately 30% greater than that required for the true 90° pulse" (7), i.e., $\alpha \approx 117^\circ$, which is very close to the theoretical value of $\alpha = 120^\circ$ reported for ideal pulses in Hahn's classic "Spin Echoes" paper (10). Consequently it was suggested that RF pulses could be calibrated by finding the pulse duration which maximizes the amplitude of the first echo and then setting desired flip angles by scaling pulse durations accordingly. Bain and Randall used a density matrix approach and ideal "delta function" pulses to analyze echo intensities resulting from both $\alpha_x\text{-}\tau\text{-}[\alpha_y\text{-}\tau\text{-}echo\text{-}\tau]_n$ and $\alpha_x\text{-}\tau\text{-}[\alpha_x\text{-}\tau\text{-}echo\text{-}\tau]_n$ echo trains. The treatment was generalized to allow for off-resonance effects and simulations for $\alpha = 90^\circ$ were reported to be in agreement with results obtained using ideal pulses. The $\alpha_x\text{-}\tau\text{-}[\alpha_x\text{-}\tau\text{-}echo\text{-}\tau]_n$ sequence was proposed (9, 11) as a useful alternative for pulse calibration since the observed "up-down" modulation of the echo amplitudes depends on α , with "3up-3down" corresponding to $\alpha = 60^\circ$ and "2up-2down" corresponding to $\alpha = 90^\circ$. Bodart *et al.* (12) discussed the merits of the two approaches and opted to perform calibration using the $90_x\text{-}\tau\text{-}[90_x\text{-}\tau\text{-}echo\text{-}\tau]_n$ sequence which, by comparison with a simulated "2up-2down" echo pattern, enabled a 90° pulse duration of 4.7 μs to be determined with a precision that was reported to be better than 0.5 μs (i.e., within 10%). Bain and Randall's analysis of the $\alpha_x\text{-}\tau\text{-}[\alpha_y\text{-}\tau\text{-}echo\text{-}\tau]_n$ sequence also suggests that, for $\alpha = 90^\circ$, the amplitude ratio of the second echo to the first echo is 1.5, whereas, for the $90_x\text{-}\tau\text{-}[90_x\text{-}\tau\text{-}echo\text{-}\tau]_n$ sequence, the ratio is 0.5. Other treatments of multipulse sequences in inhomogeneous B_0 and B_1 fields have concentrated on $\alpha\text{-}\tau\text{-}[2\alpha\text{-}\tau\text{-}echo\text{-}\tau]_n$ type sequences and include those of Hürlimann and Griffin (13), Bălibanu *et al.* (14) and Hürlimann (15).

In this paper we use the GAMMA magnetic resonance simulation platform (16) to calculate STRAFI $\alpha_x\text{-}\tau\text{-}[\alpha_y\text{-}\tau\text{-}echo\text{-}\tau]_n$ and $\alpha_x\text{-}\tau\text{-}[\alpha_x\text{-}\tau\text{-}echo\text{-}\tau]_n$ responses using a density matrix approach that takes into account the change in the effective flip angle and the phase of the signal across the selected slice.

¹ A preliminary account of some of this work was presented at the 41st Experimental Nuclear Magnetic Resonance Conference, Asilomar, 2000.

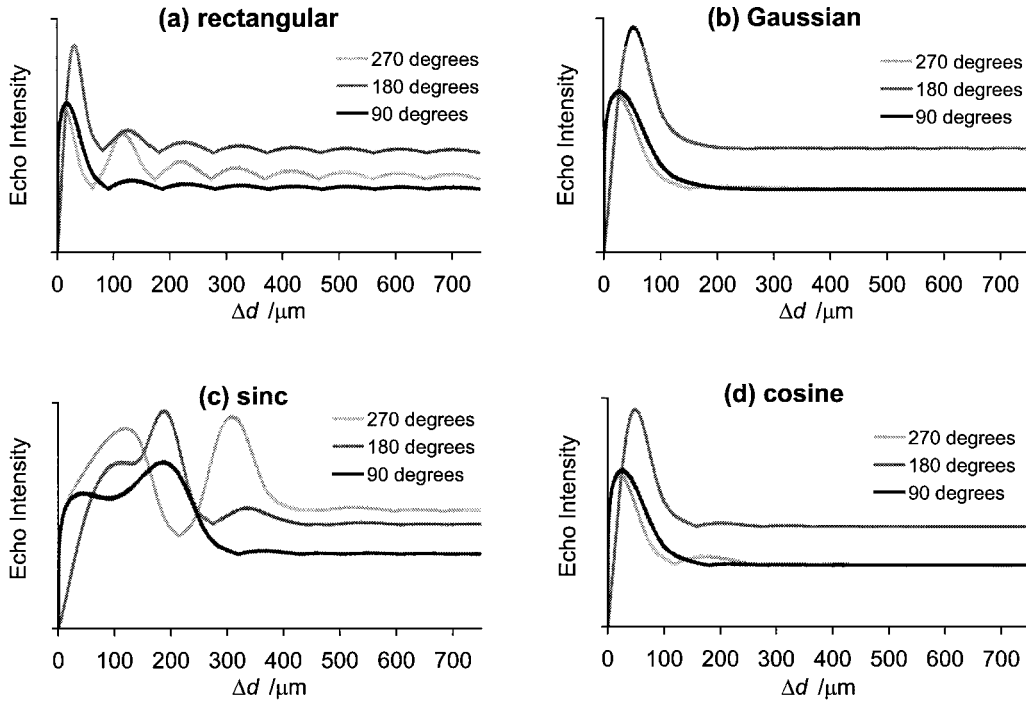


FIG. 1. Calculated intensity of the first echo in the $\alpha_x\text{-}\tau\text{-}[\alpha_y\text{-}\tau\text{-echo-}\tau]_n$ sequence as a function of Δd for $\alpha = 90^\circ, 180^\circ$ and 270° flip angles. The simulation used a single proton with Larmor frequency $\Omega/2\pi = 300$ MHz in a gradient $G = 50$ T/m. The pulses were of duration $t_p = 10$ μs and varied in shape as: (a) rectangular (b) 101 step Gaussian (cut-off at $0.02 \times$ maximum B_1) (c) 101 step sinc (cut-off at 3 nodes on both sides of maximum B_1) and (d) 101 step cosine ($1 + \cos \beta$ with β ranging $[-\pi, +\pi]$). Other parameters were the number of subsystems per micrometer ($NSS/\Delta d$) = 50, the echo time = 5000 μs , the acquisition time = 2000 μs , and the number of complex echo points = 8000. Long echo and acquisition times were used to enable computation at very small Δd values.

Calculations are performed over a specified distance, Δd , about the on-resonance condition. The computation is broken down into a specified number of subsystems (NSS) spanning Δd , each with its own characteristic flip angle, phase, and static B_0 field when the gradient is finite in the simulation. The distance Δd is typically chosen to be greater than the thickness of the excited slice. The total STRAFI response is calculated by summing the results from each of the individual subsystems. The platform is flexible and can readily employ shaped pulses.

RESULTS AND DISCUSSION

As a first step in investigating pulse angle calibration we revisit the issue of slice thickness. The selected slice for 90° rectangular pulses was reported to be essentially the distance spanned by the central lobe of the sinc excitation envelope (7). The theoretical treatment to determine Δr presented therein can be readily extended for arbitrary flip angle α (radians) to give

$$\Delta r = \frac{2 \times \sqrt{(m\pi)^2 - \alpha^2}}{\gamma t_p G}, \quad [1]$$

where m is the smallest integer satisfying $m\pi > \alpha$, and γ is the magnetogyric ratio. The distance covered by the inclusion of additional lobes on both sides of the central lobe is given by the

stepwise incrementation of m . For comparison, we have simulated the intensity of the first echo for the $\alpha_x\text{-}\tau\text{-}[\alpha_y\text{-}\tau\text{-echo-}\tau]_n$ sequence as a function of distance Δd for rectangular, Gaussian, sinc, and cosine pulses of duration (t_p) 10 μs in a STRAFI gradient (G) of 50 T/m using a Larmor frequency $\Omega/2\pi = 300$ MHz (Fig. 1).

Equation [1] satisfactorily explains why the minima for the different values of α in Fig. 1a progressively align as Δd encompasses higher values of m , however the calculations suggest that the width of the central lobe given by Eq. [1] ($m = 1, \alpha = \pi/2$), and corresponding to 40.7 μm under the conditions employed, may not be a suitable measure of the thickness of the slice excited by a 90° pulse. Indeed, if presaturation of a neighboring slice is a concern, it would perhaps be preferable to include an additional lobe on each side of the central lobe ($m = 2, \alpha = \pi/2$) corresponding to 91.0 μm under the conditions employed. For flip angles of less than 270° we have chosen, based on Fig. 1, to perform calculations with Δd set to $20\pi/\gamma t_p G$ for rectangular and sinc pulse shapes (469.7 μm in the figure) and $12\pi/\gamma t_p G$ for Gaussian and cosine pulse shapes (281.8 μm in the figure) respectively, so that all significant contributions to echo intensity are included.

Figure 2 shows the calculated first echoes for $\alpha = 90^\circ, 135^\circ$, and 180° rectangular pulses in the $\alpha_x\text{-}\tau\text{-}[\alpha_y\text{-}\tau\text{-echo-}\tau]_n$ sequence, as a function of acquisition time that is centered about the

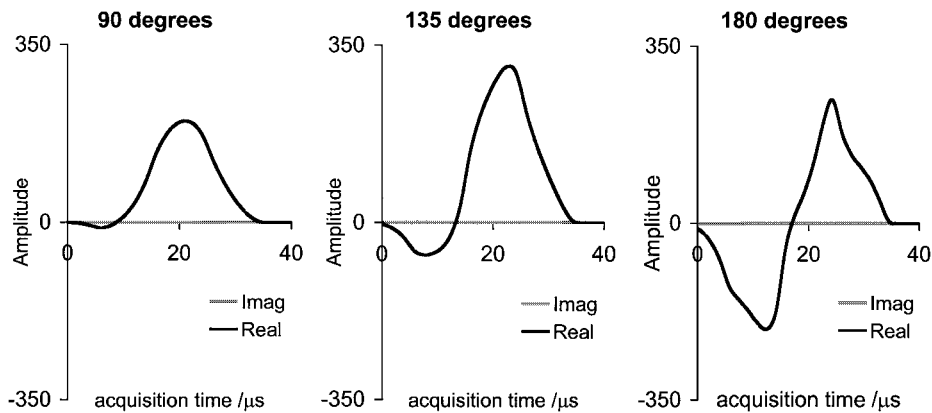


FIG. 2. Calculated first echoes for $\alpha = 90^\circ$, 135° , and 180° rectangular pulses using the $\alpha_x\text{-}\tau\text{-}[\alpha_y\text{-}\tau\text{-echo-}\tau]_n$ sequence. Isotope = ^1H , $\Omega/2\pi = 300$ MHz, $G = 50$ T/m, $NSS = 10001$, $\Delta d = 469.7$ μm , $t_p = 10$ μs , echo time = 200 μs , acquisition time = 40 μs , number of complex echo points = 2001 .

theoretical echo time. Two key features that can be attributed to the echoes are the maximum amplitude, A_{\max} , and minimum amplitude, A_{\min} . Figure 3 shows calculated contour plots of the quantities A_{\max} , $A_{\text{diff}} = A_{\max} - A_{\min}$, and $A_{\text{ratio}} = -A_{\min}/A_{\max}$ for rectangular pulses as the flip angle is varied from $\alpha = 90^\circ$ to $\alpha = 270^\circ$ in 1° steps and for pulse durations $t_p = 0.001$ μs , $t_p = 0.1$ μs to $t_p = 1$ μs in 0.1 μs steps and $t_p = 1.5$ μs to $t_p = 20$ μs in 0.5 μs steps. Δd was fixed to 469.7 μm , the value we have chosen to include all significant echo intensity contributions for 10 μs duration pulses with flip angles less than 270° under the conditions employed. Fixing Δd in this manner provides confirmation that our choice of Δd is indeed suitable for 10 μs pulses. For $t_p > 10$ μs it demonstrates that the results presented are independent of the relationship between Δd and t_p used in the simulations. Furthermore, a check on the validity of the simulations is given by the results as t_p approaches zero, which should correspond to theoretical predictions for ideal pulses. In the plots of A_{\max} and A_{diff} , data for each pulse duration were scaled to give a maximum value of 100 . Figure 4 shows the corresponding plots for Gaussian pulse shapes. Corresponding simulations to those presented in Figs. 3 and 4 were performed for sinc and cosine shaped pulses. The key features for all four pulse types are summarized in Table 1.

The calculated A_{\max} values in Figs. 3 and 4 show that the maximum echo amplitude for rectangular and Gaussian pulses correspond to flip angles of 140° and 136° respectively when all significant echo contributions are included in the calculation. These plots reveal that values greater than 95% of the maximum echo amplitude cover a range of about 38° for rectangular pulses and about 32° for Gaussian pulses, and values greater than 99.7% of the maximum echo amplitude cover an 8° range in both cases. As such, it would seem to be inherently difficult to set pulse flip angles accurately according to the pulse power that corresponds to the maximum echo amplitude under STRAFI conditions. Furthermore, the common practice of assuming that the maximum amplitude of the first echo generated by rectangular pulses cor-

responds to a 120° flip angle is expected to produce an error of about 14%.

Additional GAMMA simulations using rectangular pulses, $t_p = 10$ μs , echo time = 120 μs , and α ranging $[0^\circ, 180^\circ]$ were restricted to span only the central lobe of the sinc excitation envelope using $\Delta d = 40.7$ μm . Plots of the maximum echo amplitude and the amplitude of the echo at the theoretical echo time (te) = 120 μs were compared with the plot of the calculated first echo amplitude presented by Benson and McDonald (7). Table 2 details some characteristic features of the plots, namely the value of α corresponding to the maximum, the range of α with values greater than 95% of the maximum, and the ratio of the value at $\alpha = 180^\circ$ to the maximum value. The values reported for the plot presented by Benson and McDonald (7) are those we have estimated.

The data presented by Benson and McDonald (7) appear to agree most closely to our plots of the amplitude of the echo at the theoretical echo time (corresponding to 20 μs from the start of acquisition in the echoes of Fig. 2). Although at low flip angles the calculated echo maximum is very close to the theoretical echo time, experimentally the signal is usually passed through a low-pass filter which not only increases the signal-to-noise ratio but also delays the response somewhat in time. Indeed, at higher flip angles, acquisition of a single point at the theoretical echo time could result in no signal at all. It would, therefore, seem preferable to acquire several data points that describe the echo shape. Moreover, it is evident from the calculations that the sample regions outside the central lobe of the sinc excitation envelope make a significant contribution to the overall echo amplitude.

The calculated maximum A_{diff} values in Figs. 3 and 4 for rectangular and Gaussian pulses correspond to flip angles of 195° and 175° , respectively, when all significant echo contributions are included in the calculation, and are even less sensitive than A_{\max} to flip angle variation about the maximum. Consequently, they are not particularly useful for pulse

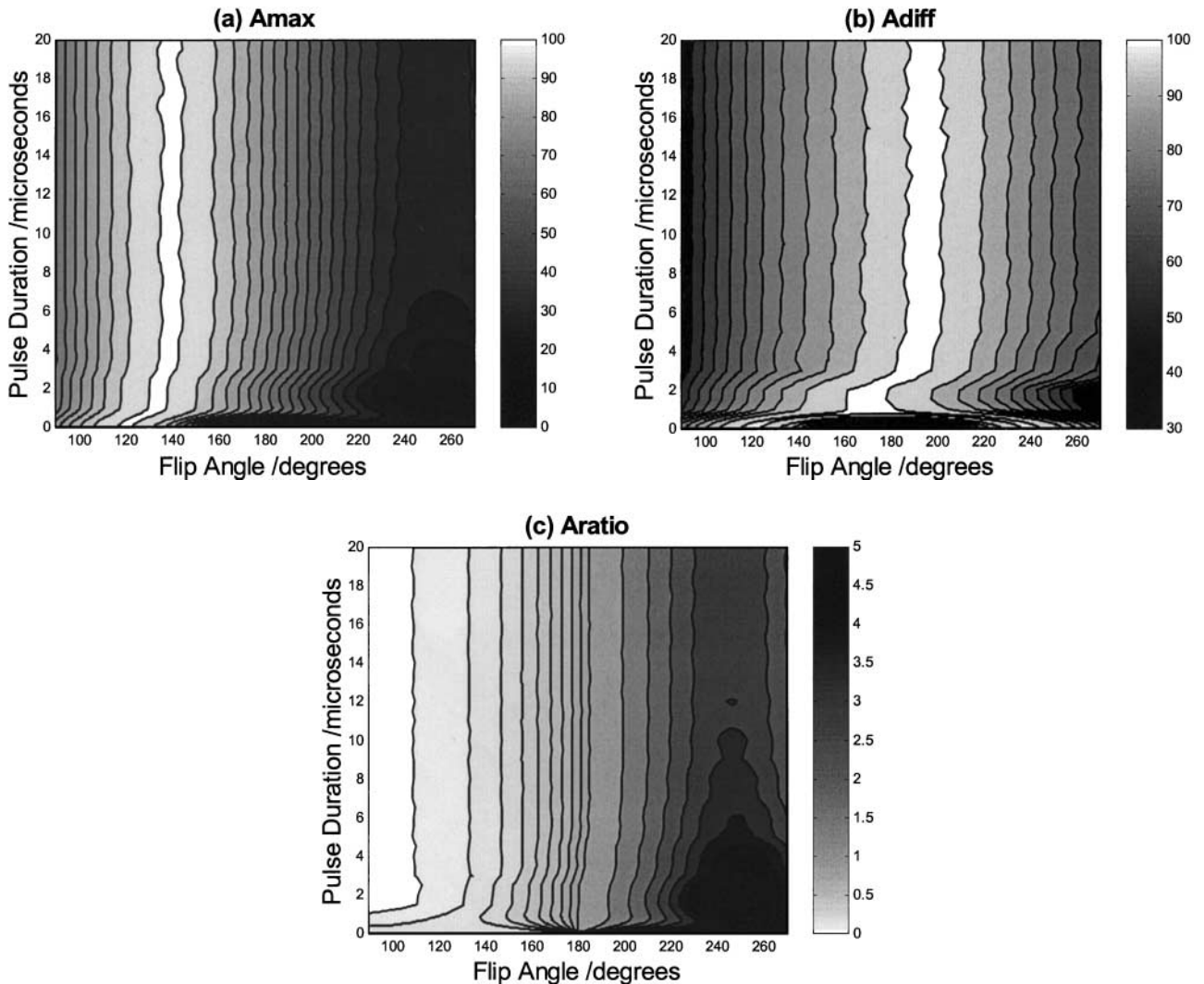


FIG. 3. Calculated quantities for the first echo in the $\alpha_x\text{-}\tau\text{-}[\alpha_y\text{-}\tau\text{-}echo\text{-}\tau]_n$ sequence using rectangular pulses. (a) A_{\max} , (b) $A_{\text{diff}} = A_{\max} - A_{\min}$, and (c) $A_{\text{ratio}} = -A_{\min}/A_{\max}$ as a function of flip angle and pulse length. The flip angle α spanned $[90^\circ, 270^\circ]$ and was incremented in 1° steps. The pulse duration t_p spanned $(0.001 \mu\text{s}, 20 \mu\text{s})$ in $0.1 \mu\text{s}$ steps from $t_p = 0.1 \mu\text{s}$ to $t_p = 1 \mu\text{s}$, and in $0.5 \mu\text{s}$ steps from $t_p = 1.5 \mu\text{s}$ to $t_p = 20 \mu\text{s}$. For A_{\max} and A_{diff} , data at each pulse duration were scaled to give a maximum value of 100. Isotope = ^1H , $\Omega/2\pi = 300 \text{ MHz}$, $G = 50 \text{ T/m}$, $NSS = 1001$, $\Delta d = 469.7 \mu\text{m}$, echo time = $250 \mu\text{s}$, acquisition time = $8t_p$ for $t_p \leq 10 \mu\text{s}$ and $80 \mu\text{s}$ for $t_p > 10 \mu\text{s}$, number of complex echo points = 2001. Contour levels (a) 10 to 95 in steps of 5 and 99.7 (b) 10 to 95 in steps of 5 and 99.5 (c) 0.1 to 1 in steps of 0.1 and 1.5 to 10 in steps of 0.5.

calibration. Conversely, the calculated A_{ratio} values (Figs. 3 and 4 and Table 1) are very sensitive to the flip angle variation, and the sensitivity appears to increase with flip angle over the range studied.

Experiments to test the calculated A_{ratio} results were performed at $\Omega/2\pi = 111.5 \text{ MHz}$ in an accurately calibrated gradient of $12.091 \pm 0.016 \text{ T/m}$ (17). Figure 5 shows the experimental and calculated amplitudes of the first echo in the $\alpha_x\text{-}\tau\text{-}[\alpha_y\text{-}\tau\text{-}echo\text{-}\tau]_n$ sequence as a function of rectangular pulse duration t_p for the rubber component in a compartmentalized water–rubber–PMMA phantom using a filter bandwidth (fb) of 2000 Hz. The filter eliminates contributions to the echoes other than those with

essentially uniform flip angle from a very thin slice about the on-resonance condition. This provides an accurate means of pulse calibration, similar to that routinely employed in conventional NMR, and gives $t_p = 91 \pm 1 \mu\text{s}$ for $\alpha = 360^\circ$. The calculated echo amplitudes with $t_p = 91 \mu\text{s}$ corresponding to $\alpha = 360^\circ$, and $\Delta d = 7.77 \mu\text{m}$ (corresponding to 4000 Hz about the on-resonance condition) are in reasonable agreement with the experimental results considering that the calculation represents the application of a perfect low-pass filter. Narrow filter bandwidths can be used to improve the spatial resolution in STRAFI imaging experiments, but the trade-off is the longer rise time of the signal response which delays acquisition. Figure 6 shows

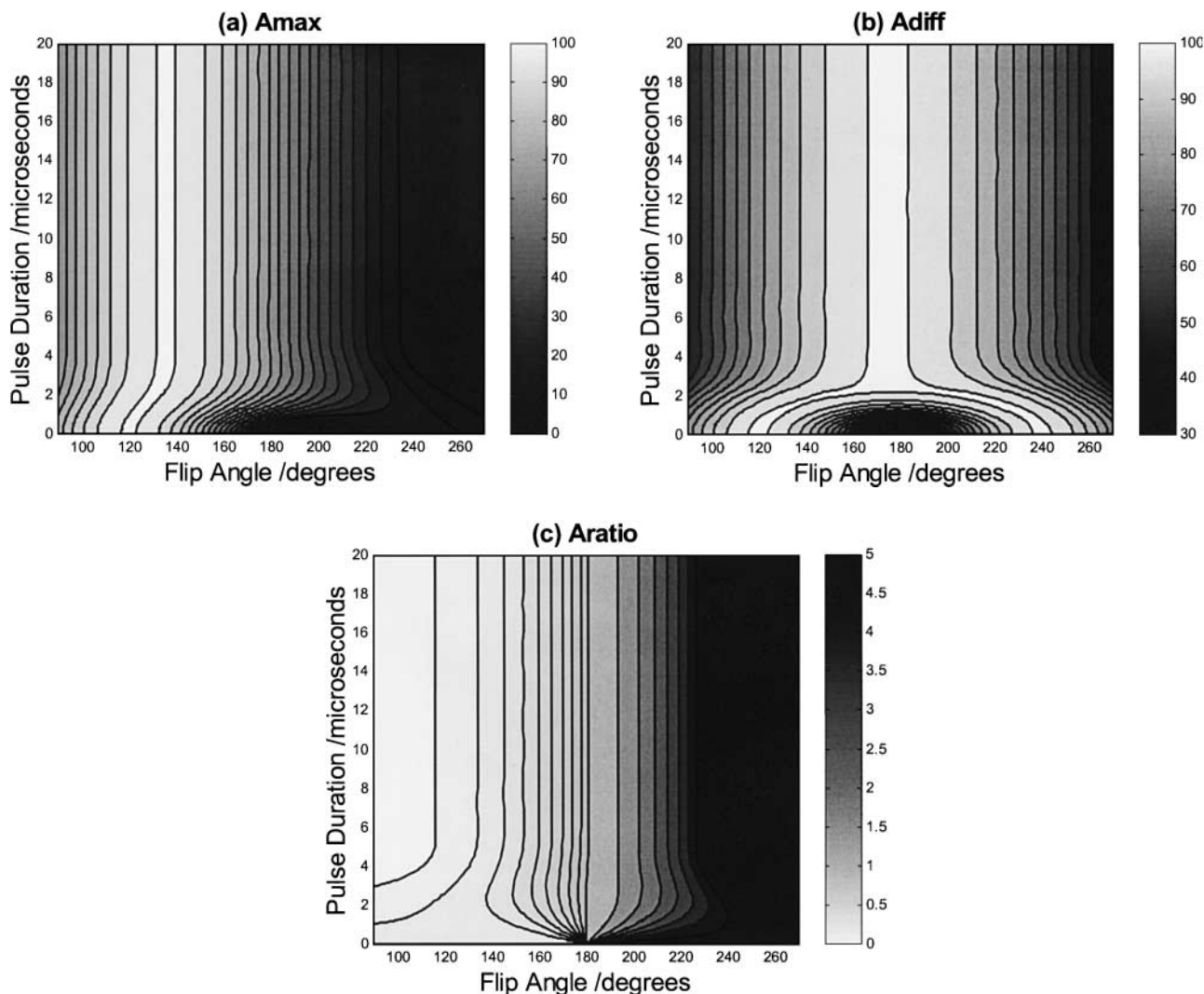


FIG. 4. Calculated quantities for the first echo in the $\alpha_x\text{-}\tau\text{-}[\alpha_y\text{-}\tau\text{-}echo\text{-}\tau]_n$ sequence using 101 step Gaussian pulses (cut-off at $0.02 \times$ maximum B_1). (a) A_{\max} , (b) $A_{\text{diff}} = A_{\max} - A_{\min}$ and (c) $A_{\text{ratio}} = -A_{\min}/A_{\max}$ as a function of flip angle and pulse length. The flip angle α spanned $[90^\circ, 270^\circ]$ and was incremented in 1° steps. The pulse duration t_p spanned $(0.001 \mu\text{s}, 20 \mu\text{s})$ in $0.1 \mu\text{s}$ steps from $t_p = 0.1 \mu\text{s}$ to $t_p = 1 \mu\text{s}$, and in $0.5 \mu\text{s}$ steps from $t_p = 1.5 \mu\text{s}$ to $t_p = 20 \mu\text{s}$. For A_{\max} and A_{diff} , data at each pulse duration were scaled to give a maximum value of 100. Isotope = ^1H , $\Omega/2\pi = 300 \text{ MHz}$, $G = 50 \text{ T/m}$, $NSS = 1001$, $\Delta d = 281.8 \mu\text{m}$, echo time = $250 \mu\text{s}$, acquisition time = $8t_p$ for $t_p \leq 10 \mu\text{s}$ and $80 \mu\text{s}$ for $t_p > 10 \mu\text{s}$, number of complex echo points = 2001. Contour levels (a) 10 to 95 in steps of 5 and 99.7 (b) 10 to 95 in steps of 5 and 99.5 (c) 0.1 to 1 in steps of 0.1 and 1.5 to 10 in steps of 0.5.

results for the rubber from a more conventional STRAFI experiment using $fb = 256,000 \text{ Hz}$. The A_{ratio} values measured experimentally for each component of the phantom at specific t_p values close to 90° , 120° , 135° , and 180° are summarized in Table 3.

The experimental A_{ratio} results for the rubber sample (Table 3) are in excellent agreement with the calculated values (Table 1) and suggest that the A_{ratio} value for a 180° pulse (0.861 for rectangular pulses) can be used to accurately calibrate pulses on a suitable sample, such as rubber, to within 1% accuracy. A table of calculated A_{ratio} values for rectangular pulses with α ranging $[90^\circ, 270^\circ]$ in 1° steps is available at

<http://xenon.chem.qmul.ac.uk/acrobat/Aratio.pdf>. Fast and accurate calibration can be achieved by estimation of the flip angle from an initial experiment and subsequent adjustment of pulse power or duration to “home in” on the A_{ratio} value for a 180° pulse.

Experimental A_{ratio} values were measured for tap water and PMMA components in the same phantom, which were chosen to be representative of samples with a high self diffusion coefficient and a short T_2 relaxation time, respectively. The results for water are in fairly good agreement with simulation, and we estimate that pulse calibration using the A_{ratio} method on water is accurate to within 2%. The slightly lower A_{ratio} values in

TABLE 1
Averaged Features of the 2D Plots of A_{\max} , A_{diff} , and A_{ratio} for $t_p \geq 10 \mu\text{s}$ for Rectangular (Fig. 3), Gaussian (Fig. 4), Sinc, and Cosine Shaped Pulses

Feature	Pulse shape			
	Rectangular	Gaussian	Sinc ^b	Cosine
Maximum A_{\max} ^a	$139.8^\circ \pm 1.1^\circ$	$136.0^\circ \pm 0.0^\circ$	$130^\circ \pm 0.0^\circ$	$135^\circ \pm 0.0^\circ$
Maximum A_{diff} ^a	$195.0^\circ \pm 1.0^\circ$	$175.0^\circ \pm 0.0^\circ$	$131.0^\circ \pm 0.0^\circ$ ^c	$173.0^\circ \pm 0.0^\circ$
A_{ratio} at 90°	0.056 ± 0.001	0.0296 ± 0.0001	0.2207 ± 0.0001	0.0351 ± 0.0001
A_{ratio} at 120°	0.137 ± 0.001	0.1158 ± 0.0001	0.2197 ± 0.0001	0.1237 ± 0.0001
A_{ratio} at 135°	0.210 ± 0.001	0.2070 ± 0.0001	0.2257 ± 0.0001	0.2154 ± 0.0001
A_{ratio} at 150°	0.329 ± 0.001	0.3545 ± 0.0001	0.2582 ± 0.0001	0.3631 ± 0.0001
A_{ratio} at 180°	0.861 ± 0.003	0.9657 ± 0.0002	0.6389 ± 0.0002	0.9747 ± 0.0002

^a The errors given for A_{\max} and A_{diff} are based on calculations performed at 1° intervals. This was sufficient resolution to produce a variation in results for rectangular pulses, but not in results for the other pulse shapes studied.

^b The results for sinc shaped pulses reflect the calculated echo shapes which have several local maxima and minima even at relatively small flip angles.

^c There is another local maximum at $265.0^\circ \pm 0.0^\circ$ with A_{diff} approximately 95% of the maximum at $131.0^\circ \pm 0.0^\circ$.

water were observed to be reproducible on successive measurements, and perhaps this can be attributed to the effect of self diffusion. It is, however, possible that slightly longer pulse durations are genuinely required for the tap water component of the phantom due to RF penetration effects. The effect of self diffusion on the A_{ratio} value can be estimated from the coefficient for signal attenuation in the presence of a steady gradient (18),

$$\overline{\exp(i\Delta\phi)} = \exp\left(-\frac{1}{3}\gamma^2 G^2 D t^3\right), \quad [2]$$

in which D is the self diffusion coefficient $= 2.3 \times 10^{-9} \text{ m}^2/\text{s}$ for water (19), and $t = t_{\text{Amax}} - t_{\text{Amin}}$. We have observed experimentally that $t_{\text{Amax}} - t_{\text{Amin}} \approx 1.2 \times t_p$ for 180° pulses, and simulated results are in good agreement (Fig. 2 shows an example). As such, we estimate that, relative to A_{min} , A_{max} is attenuated by a

TABLE 2
Features of Calculated Amplitudes for α Ranging $[0^\circ, 180^\circ]$ in Steps of 1° . $t_p = 10 \mu\text{s}$ Rectangular Pulses, Echo Time = $120 \mu\text{s}$

Calculated plot (as a function of α)	Feature		
	Value of α corresponding to the maximum	Range of α with values >95% of the maximum	Ratio of value at $\alpha = 180^\circ$ to the maximum value
A_{\max} , $\Delta d = 40.7 \mu\text{m}$ Echo amplitude	130°	34°	0.67
at $t_e, \Delta d = 40.7 \mu\text{m}$	125°	29°	0.29
A_{\max} , $\Delta d = 469.7 \mu\text{m}$ Echo amplitude	140°	38°	0.79
at $t_e, \Delta d = 469.7 \mu\text{m}$	126°	28°	0.31
Benson and McDonald (7)	128°	28°	0.34

factor of 0.9986 for $t_p = 45.5 \mu\text{s}$ and $G = 12.091 \text{ T/m}$, and that the resulting A_{ratio} values are accurate to within less than 0.2%. The PMMA A_{ratio} results are severely distorted by the fast T_2 relaxation which was measured to be $36 \pm 4 \mu\text{s}$ by exponential fitting of the maximum amplitude of the first echo as a function of echo time. Clearly the A_{ratio} method is not suitable for samples that exhibit significant T_2 relaxation relative to the timescale of the measurement. The T_2 of the rubber sample was measured to be $4.3 \pm 0.4 \text{ ms}$.

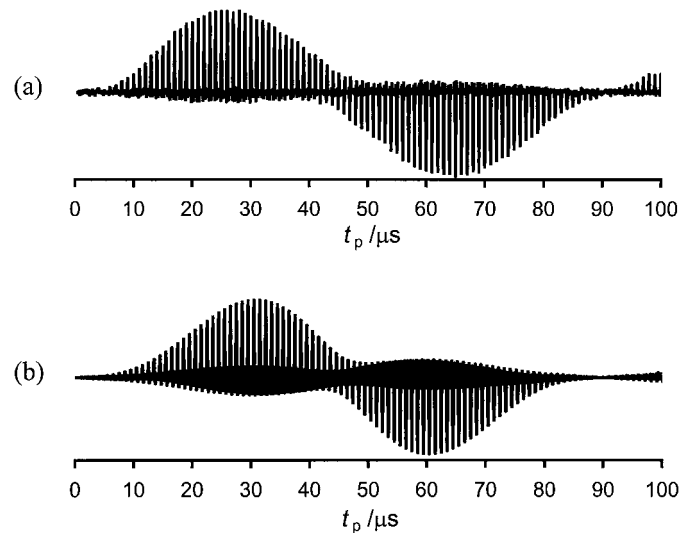


FIG. 5. Experimental and simulated first echoes in the $\alpha_x\text{-}\tau\text{-}[\alpha_y\text{-}\tau\text{-}echo\text{-}\tau]_n$ sequence as a function of rectangular pulse duration t_p for a rubber bung. Isotope = ^1H , $\Omega/2\pi = 111.5 \text{ MHz}$, $G = 12.091 \pm 0.016 \text{ T/m}$, echo time = $2500 \mu\text{s}$, sampling interval = $25 \mu\text{s}$, number of complex points per echo = 128, acquisition time = $1600 \mu\text{s}$. (a) Experimental: filter bandwidth = 2000 Hz , repetition time = 1 s , number of transients = 512. (b) Simulated: $NSS = 1001$, $\Delta d = 7.77 \mu\text{m}$.

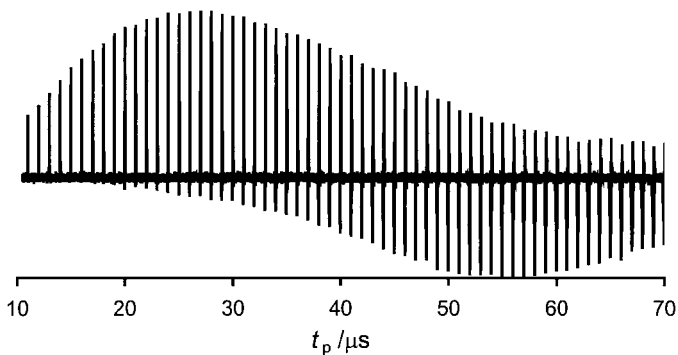


FIG. 6. Experimental first echo in the $\alpha_x\text{-}\tau\text{-}[\alpha_x\text{-}\tau\text{-echo-}\tau]_n$ sequence as a function of rectangular pulse duration t_p for a rubber bung. Isotope = ^1H , $\Omega/2\pi = 111.5$ MHz, $G = 12.091 \pm 0.016$ T/m, echo time = 1000 μs , filter bandwidth = 256000 Hz, sampling interval = 2 μs , number of complex points per echo = 384, acquisition time = 768 μs , repetition time = 1 s, number of transients = 512.

Accurate pulse calibration using the $\alpha_x\text{-}\tau\text{-}[\alpha_x\text{-}\tau\text{-echo-}\tau]_n$ echo train requires comparison with simulated echo trains due to the way in which the individual echo components combine. To our knowledge the simulated echo train has been published only for $\alpha = 90^\circ$ (12). The method has not found general use, presumably because the sensitivity of the echo train to flip angle variation is not well documented. Figure 7 depicts the simulated results for flip angles about $\alpha = 90^\circ$. Figure 8 shows the experimental results for the rubber component using rectangular pulses with $t_p = 21.4875, 21.7375, 21.9875, 22.25, 22.5, 22.75, 23, 23.25, 23.5125,$ and 23.7625 μs which corresponds to α ranging $[85^\circ, 94^\circ]$ in 1° steps as deter-

TABLE 3
Experimental A_{ratio} Values for Rubber, Tap Water, and PMMA

$\alpha/^\circ$	$t_p/\mu\text{s}$	A_{ratio}		
		Rubber	Tap water	PMMA
87.0	22.0	0.0490	0.0417	0.6644
89.0	22.5	0.0516	0.0466	0.7552
91.0	23.0	0.0635	0.0508	0.7589
116.7	29.5	0.1262	0.1187	2.1033
118.7	30.0	0.1341	0.1260	2.1421
120.7	30.5	0.1481	0.1347	2.4231
132.5	33.5	0.2037	0.1858	3.2607
134.5	34.0	0.2094	0.1955	3.2975
136.5	34.5	0.2295	0.2074	3.4360
178.0	45.0	0.8105	0.7278	6.3850
179.0	45.25	0.8393	0.7783	^a
180.0	45.5	0.8573	0.8061	6.4083
181.0	45.75	0.8829	0.8294	^a
182.0	46.0	0.9244	0.8490	6.7324
183.0	46.2625	0.9396	0.8713	^a

Note. The values of α correspond to those determined by the filtered experiment on the rubber component shown in Fig. 5a.

^a Value not determined.

mined by the filtered experiment and confirmed by the A_{ratio} method.

The simulated $\alpha_x\text{-}\tau\text{-}[\alpha_x\text{-}\tau\text{-echo-}\tau]_n$ echo trains (Fig. 7) are very sensitive to flip angle. In particular, it appears that the maximum amplitudes of the 3rd and 4th echoes can readily be used for pulse calibration. The maximum echo amplitudes are equal to within 3% for $\alpha = 90^\circ$ and to within 1% for $\alpha = 91^\circ$. Additional calculations show that the maximum echo amplitudes are equal to within 0.04% for $\alpha = 90.75^\circ$. As with the A_{ratio} method, relaxation effects have not been accounted for, so the method relies on negligible relaxation over the timescale of the measurement. The experimental results on the rubber component (Fig. 8) are in very good agreement. Experiments on the tap water component that were performed under identical conditions (other than a repetition time of 15 s) could not be used for pulse calibration due to the effect of self diffusion over the time scale of the experiment (echo time = 250 μs). Indeed, the maximum amplitude of the 4th echo was observed to be less than that of the 3rd echo over the entire range of t_p values corresponding to α ranging $[85^\circ, 94^\circ]$ in 1° steps for the rubber component.

Simulated $\alpha_x\text{-}\tau\text{-}[\alpha_y\text{-}\tau\text{-echo-}\tau]_n$ echo trains were observed to give a value of 1.59 for the amplitude ratio of the second echo to the first echo for $\alpha = 90^\circ$, with a variation of about 0.6% in the ratio per degree about $\alpha = 90^\circ$. This compares to a variation of about 3% in A_{ratio} values per degree about $\alpha = 180^\circ$.

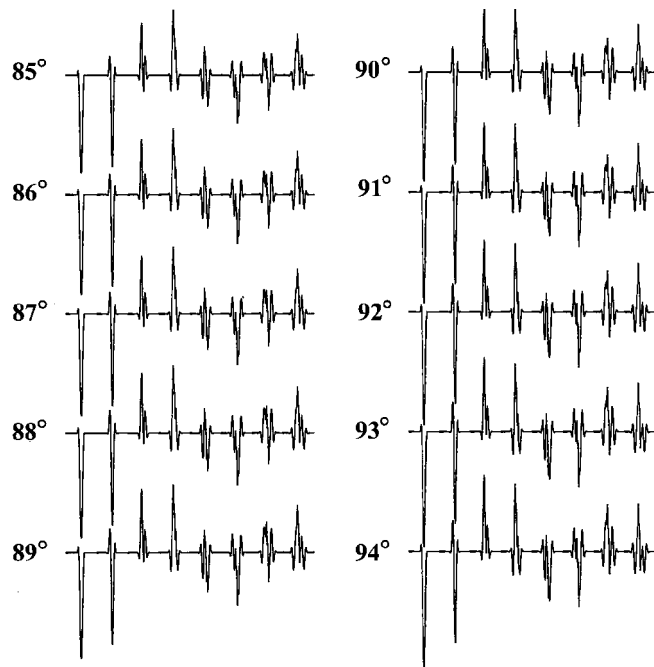


FIG. 7. Calculated echo trains for rectangular pulses with α ranging $[85^\circ, 94^\circ]$ in 1° steps for the $\alpha_x\text{-}\tau\text{-}[\alpha_x\text{-}\tau\text{-echo-}\tau]_n$ sequence, $n = 8$. Isotope = ^1H , $\Omega/2\pi = 300$ MHz, $G = 50$ T/m, $NSS = 10001$, $\Delta d = 469.7$ μm , $t_p = 10$ μs , echo time = 250 μs , acquisition time per echo = 150 μs , number of complex points per echo = 301.

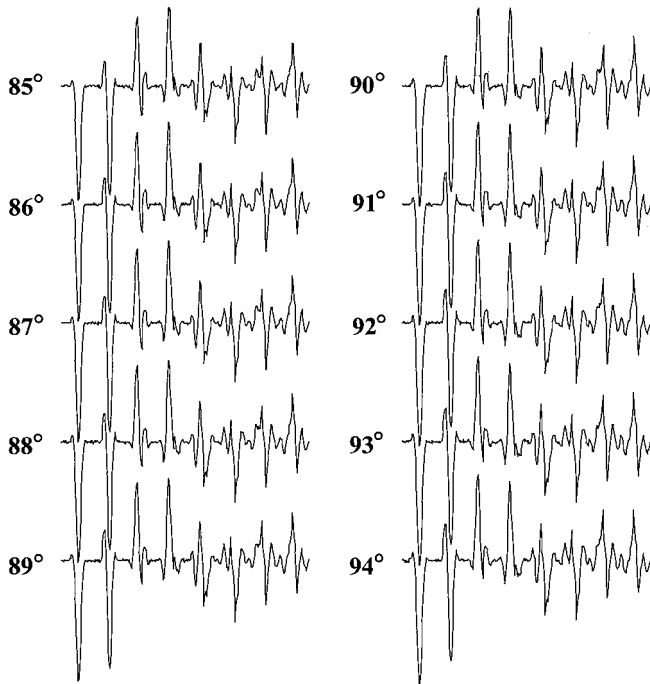


FIG. 8. Experimental echo trains for a rubber bung using rectangular pulses with α ranging $[85^\circ, 94^\circ]$ in 1° steps ($t_p = 21.4875, 21.7375, 21.9875, 22.25, 22.5, 22.75, 23, 23.25, 23.5125, \text{ and } 23.7625 \mu\text{s}$ respectively as determined by the filtered experiment and confirmed by the A_{ratio} method) for the $\alpha_x - \tau - [\alpha_x - \tau - \text{echo} - \tau]_n$ sequence, $n = 8$. Isotope = ^1H , $\Omega/2\pi = 111.5 \text{ MHz}$, $G = 12.091 \pm 0.016 \text{ T/m}$, echo time = $250 \mu\text{s}$, filter bandwidth = $256,000 \text{ Hz}$, sampling interval = $2 \mu\text{s}$, number of complex points per echo = 160, acquisition time per echo = $160 \mu\text{s}$, repetition time = 1 s , number of transients = 512.

CONCLUSIONS

It is now possible to calibrate pulses for STRAFI echo trains accurately to within 1% in a simple manner on samples that exhibit negligible T_2 relaxation and self diffusion over a timescale that is the order of the pulse duration using the A_{ratio} method for π pulses. For samples that exhibit a high self diffusion coefficient, such as water, the A_{ratio} method appears to remain accurate under typical STRAFI conditions. The A_{ratio} method is more robust than calibration with the $\alpha_x - \tau - [\alpha_x - \tau - \text{echo} - \tau]_n$ sequence which gives the same degree of accuracy, but only on samples that exhibit negligible relaxation and self diffusion over a timescale that is on the order of the echo time used. For samples that exhibit significant T_2 relaxation over a timescale that is on the order of the pulse duration, it may be desirable to include a strip of a suitable material along with the sample for accurate pulse calibration. Given that accurate pulse calibration can be performed, a quantitative analysis of echo train intensities according to the relaxation properties of a sample should now be possible. The GAMMA platform includes relaxation treatments and their use in STRAFI echo train calculations are now under investigation.

EXPERIMENTAL

Experiments were performed at 111.5 MHz on a Varian UNITYInova high-resolution imaging spectrometer equipped with a 4.7 T, 33 cm horizontal bore Oxford Instruments superconducting magnet. A probe that can take samples up to 5 cm in diameter and 8 cm long (20) was used to test the calculated results in an accurately calibrated STRAFI gradient of $12.091 \pm 0.016 \text{ T/m}$ (17).

COMPUTATIONAL

The GAMMA magnetic resonance simulation platform (16) was used for all calculations presented. In the absence of diffusion, system evolution through a STRAFI pulse train is taken to be the summed result over a specified number of subsystems per unit length in the applied gradient. Each subsystem, which can contain any number of spins of any isotope type, experiences a specific external field. These may be evolved through virtually any pulse sequence using density operator formalism, and such evolutions are amenable to the full machinery available in the platform: shaped pulses, relaxation, spin and spin-spin interactions, and powder averaging. For this investigation we have examined only a single proton without including relaxation effects. Care was taken to ensure system response was accurately modeled by repeating simulations at differing subsystem densities (subsystems/ μm) and including all subsystems that significantly contribute to echo intensity. The statement “`#include <gamma.h>`” is all that is required to access the STRAFI functionality. An example GAMMA simulation program that gives the output for 135° rectangular pulses in Fig. 2 is given below. Additional examples and specific documentation may be found at <http://gamma.magnet.fsu.edu/examples/strafi/> and <http://gamma.magnet.fsu.edu/pdf/strafi/>, respectively.

```
#include <gamma.h> // include GAMMA
int main() {
    sys_gradz sys(1); // set single spin in a z-gradient
    sys.Omega(300.0); // set field strength to 300 MHz
    sys.BoGrad(50.0); // set z-gradient to 50 T/m
    sys.SysLen(469.7*1.e-6); // set DELTAd to 469.7 microns
    sys.NSS(10001); // set # sub-systems
    int NSS=sys.NSS(); // set NSS to # sub-systems
    gen_op H=Ho(sys); // set evolution Hamiltonian
    gen_op Hs[NSS]; // set up Hamiltonians
    Hzgrad(sys,H,Hs); // fill up Hamiltonians
    string I=sys.symbol(0); // prepare to work on spin
    double tp=10.e-6; // set pulse duration to 10 us
    double pa=135.0; // set flip angle to 135 degrees
    gen_op UPxs[NSS]; // x pulse propagators
    for(int i=0; i<NSS; i++) // fill up x pulse propagators
        UPxs[i]=Sxpuls_U(sys,Hs[i],I,0,tp,pa);
    gen_op UPys[NSS]; // y pulse propagators
```

```

for(int i=0; i < NSS; i++) // fill up y pulse propagators
  UPys[i] = Sypuls.U(sys, Hs[i], I, 0, tp, pa);
double d1 = 90.e-6; // set time delay d1 to 90 us
double d2 = 75.e-6; // set time delay d2 to 75 us
gen_op Ud1s[NSS], Ud2s[NSS]; // time evolution propagators
Props(NSS, Hs, d1, Ud1s); // fill up d1 propagators
Props(NSS, Hs, d2, Ud2s); // fill up d2 propagators
gen_op sigmas[NSS]; // working density operator
gen_op sigma0 = sigma_eq(sys); // this is equilibrium
evolve(NSS, sigma0, UPxs, sigmas); // apply the x pulse
evolve(NSS, sigmas, Ud1s, sigmas); // time evolution for d1
evolve(NSS, sigmas, UPys, sigmas); // apply the y pulse
evolve(NSS, sigmas, Ud2s, sigmas); // time evolution for d2
int np = 2001; // define #points to acquire
row_vector data(np); // set storage for data
gen_op D = -Fm(sys); // set up detection operator
D = complexi*D; // set correct phase
double si = 2.e-8; // set sampling interval
for(int i=0; i < NSS; i++) {
  acquire1D ACQ(D, Hs[i]); // prepare for acquisition
  data += ACQ.T(sigmas[i], np, si); // acquire data
}
GP_1D("echo.asc", data); // output echo
}

```

ACKNOWLEDGMENTS

GAMMA is provided to the public courtesy of its authors and is supported by the National High Magnetic Field Laboratory. Detailed information and platform downloading is available at <http://gamma.magnet.fsu.edu>. We thank Andrei Samoilenko for enlightening and stimulating discussions during the course of this study. The Varian UNITYInova imaging spectrometer was provided by the ULIRS (University of London Intercollegiate Research Service) Scheme and is located at Queen Mary, University of London. This work was partially supported by the Bio-technical and Biological Science Research Council through Grant 68/E08576.

REFERENCES

1. B. Newling and P. J. McDonald, Stray field magnetic resonance imaging, *Rep. Prog. Phys.* **61**, 1441–1493 (1999).
2. P. J. McDonald, Stray field magnetic resonance imaging, *Prog. in NMR Spectrosc.* **30**, 69–99 (1997).
3. B. Geil, Measurement of translational molecular diffusion using ultrahigh

- magnetic field gradient NMR, *Concepts in Magn. Reson.* **10**, 299–321 (1998).
4. A. A. Samoilenko, D. Y. Artemov, and L. A. Sebeldina, Formation of sensitive layer in experiments on NMR subsurface imaging of solids, *JEPT Lett.* **47**, 417–419 (1988).
5. W.-K. Rhim, D. P. Burum, and D. D. Elleman, Multiple-pulse spin locking in dipolar solids, *Phys. Rev. Lett.* **37**, 1764–1766 (1976).
6. W.-K. Rhim, D. P. Burum, and D. D. Elleman, Calculation of spin-lattice relaxation during pulsed spin locking in solids, *J. Chem. Phys.* **68**, 692–695 (1978).
7. T. B. Benson and P. J. McDonald, Profile amplitude modulation in stray field magnetic resonance imaging, *J. Magn. Reson. A* **112**, 17–23 (1995).
8. T. B. Benson and P. J. McDonald, The application of spin echoes to stray-field imaging, *J. Magn. Reson. B* **109**, 314–317 (1995).
9. A. D. Bain and E. W. Randall, Hahn spin echoes in large static gradients following a series of 90° pulses, *J. Magn. Reson. A* **123**, 49–55 (1996).
10. E. L. Hahn, Spin echoes, *Phys. Rev.* **80**, 580–594 (1950).
11. E. W. Randall, A convenient method for calibration of the pulse-length in high field-gradients using Hahn echo-trains, *Solid State Nuclear Magn. Res.* **8**, 179–183 (1997).
12. P. Bodart, T. Nunes, and E. W. Randall, Stray-field imaging of quadrupolar nuclei of half integer spin in solids, *Solid State Nuclear Magn. Res.* **8**, 257–263 (1997).
13. M. D. Hürlimann and D. D. Griffin, Spin dynamics of Carr–Purcell–Meiboom–Gill-like sequences in grossly inhomogeneous B₀ and B₁ fields and application to NMR well logging, *J. Magn. Reson.* **143**, 120–135 (2000).
14. F. Bălibanu, K. Hailu, R. Eymael, D. E. Demco, and B. Blümich, Nuclear magnetic resonance in inhomogeneous magnetic fields, *J. Magn. Reson.* **145**, 246–258 (2000).
15. M. D. Hürlimann, Diffusion and relaxation effects in general stray field NMR experiments, *J. Magn. Reson.* **148**, 367–378 (2001).
16. S. A. Smith, T. O. Levante, B. H. Meier, and R. R. Ernst, Computer simulations in magnetic resonance. An object oriented programming approach, *J. Magn. Reson. A* **106**, 75–105 (1994).
17. A. R. Preston, P. Kinchesh, and E. W. Randall, Calibration of the stray field gradient by a heteronuclear method and by field profiling, *J. Magn. Reson.* **146**, 359–362 (2000).
18. P. T. Callaghan, “Principles of Nuclear Magnetic Resonance Microscopy,” p. 160, Clarendon Press, Oxford (1991).
19. M. Holz and H. Weingärtner, Calibration in accurate spin-echo self-diffusion measurements using ¹H and less-common nuclei, *J. Magn. Reson.* **92**, 115–125 (1991).
20. P. Kinchesh, A. A. Samoilenko, A. R. Preston, and E. W. Randall, STRAFI-NMR of soil water: Development of a new large probe and preliminary results, *J. Environ. Qual.* **31** (2002).